

Kinetics and mechanism of hydrolysis of *p*-nitrophenyl picolinate by transition-metal hydroxamate containing benzo-15-crown-5

Ying Tang^a, Fa-mei Feng^b, Jian-zhang Li^{b,c}, Hong-bo Li^c, Shen-xin Li^b and Sheng-ying Qin^{c,*}

^aDepartment of Chemistry, Chongqing University of Arts and Sciences, Chongqing, 402168, P. R. China

^bDepartment of Chemistry, Sichuan University of Science & Engineering, Zigong, Sichuan, 643000, P. R. China

^cDepartment of Chemistry, Sichuan University, Chengdu, Sichuan 610064, P. R. China

Two hydroxamic acids **HL**¹ and **HL**² containing benzo-15-crown-5 have been synthesised and their transition metal (Cu²⁺, Co²⁺, Zn²⁺, Mn²⁺) complexes have been employed as models to mimic hydrolase in catalytic hydrolysis of *p*-nitrophenyl picolinate (PNPP). The kinetics and mechanism of PNPP hydrolysis have been investigated. A kinetic mathematical model of PNPP cleavage catalysed by these complexes is proposed. The effects of reactive temperature and metal ion in complexes on the rate of catalytic PNPP hydrolysis are discussed. The results show that the transition-metal hydroxamates (ML₁², ML₂², M= Cu²⁺, Co²⁺, Zn²⁺, Mn²⁺) containing benzo-15-crown-5 exhibit high activity in catalytic PNPP hydrolysis. The rate of PNPP hydrolysis catalysed by these complexes increased along with the increase of pH values of the buffer solution; the catalytic activity of different metal ions in complexes of the same ligand decreased in the order Cu²⁺ > Co²⁺ > Zn²⁺ > Mn²⁺; the pseudo-first-order-rate constants of PNPP hydrolysis catalysed by the complexes are over 1000 times more than that of spontaneous hydrolysis of PNPP.

Keywords: benzo-15-crown-5, transition-mental hydroxamate, mimic hydrolase, catalytic kinetics, *p*-nitrophenyl picolinate

Metal complex catalysis in the hydrolysis of carboxyl esters and phosphoric esters is an area of active research.^{1,2} Much research has been undertaken to develop high efficiency and selective catalysts in order to achieve environmentally friendly and high-economy processes. In previous studies on the catalytic hydrolysis of carboxyl esters, many kinds of bivalent transition metal complexes, such as Cu²⁺, Zn²⁺, Co²⁺ and Mn²⁺, have been employed for PNPP hydrolysis catalysed in buffer solutions.³⁻⁵ These complexes exhibit good catalytic properties for hydrolysis of *p*-nitrophenyl picolinate (PNPP) and phosphodiester. A large number of studies on mimic hydrolytic metalloenzymes have used transition-mental complexes of macrocyclic dioxotetraamine,⁶ calixarene,⁷ cyclodextrine⁸ and Schiff base^{9,10} *etc.* artificial hydrolytic enzyme models, but use of transition-mental hydroxamates as the synthetic model has not been reported up to now.

Previously, a number of reports have appeared on the applications of hydroxamic acids as enzyme inhibitors,¹¹ artificial siderophore,^{12,13} synthetic nuclease,¹⁴ and chiral catalyst.¹⁵ We also reported the dioxygen affinities and biomimetic catalytic oxidation performance of transition-metal hydroxamates.^{16,17} We now report the synthesis of hydroxamic acid complexes containing benzo-15-crown-5 (see Fig. 1), the catalytic performance of these complexes for

PNPP hydrolysis, and the kinetics and mechanism of PNPP hydrolysis. The effects of reactive temperature and the metal ion in complexes on the rate of catalytic PNPP hydrolysis are also discussed.

Experimental

Melting points were determined on a Yanaco MP-500 micro-melting point apparatus and are uncorrected. Infrared spectra were recorded on a Nicolet-1705X spectrometer. ¹H NMR spectra were recorded on a Bruker AC-200MHz spectrometer using tetramethylsilane as internal standard. Mass spectra were obtained on a Finnigan MAT 4510 spectrometer and Finnigan LCQ-DECA spectrometer. The metal ion contents were measured by an IRIS-Advantage ICP emission spectrometer. Other elementary analysis was performed on a Carlo Erba 1106 elemental analyser. Molar conductance was obtained (in DMF solution) on a DDS-11A conductivitymeter. Kinetic studies were carried out by UV-Vis methods with a GBC 916 u.v.-vis spectrophotometer equipped with a thermostatic cell holder.

Materials

All reagents, unless otherwise indicated, were of analytical grade and were used without further purification. The water used for kinetics was obtained by doubly distilling deionised water. Buffers were made from standardised nitric acid. Tris(hydroxymethyl)aminomethane was supplied by Sigma Chemical Co. The pH value of the buffer solutions was measured at 25 °C using a Radiometer PHM 26 pH meter fitted with G202C glass and K4122 calomel electrodes.

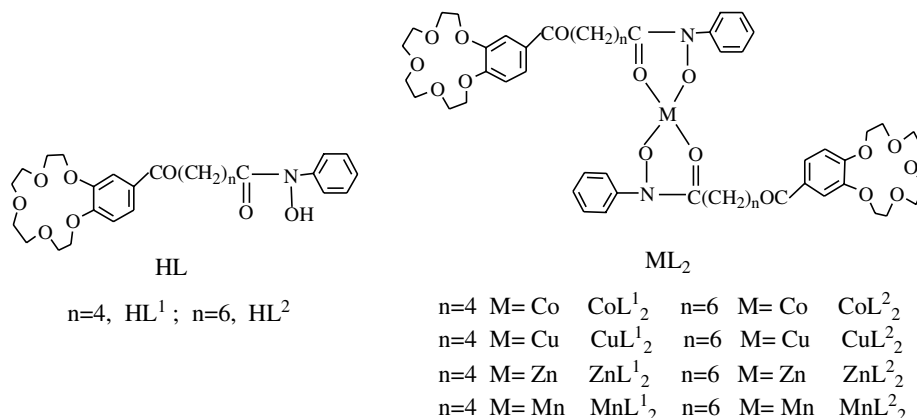


Fig. 1 Structures of hydroxamic acids and their complexes.

* Correspondent. E-mail: lyl63@sina.com

The following compounds were prepared according to the literature: *N*-phenylhydroxylamine,¹⁸ PNPP(*p*-nitrophenyl picolinate),¹⁹ 4'-(ω -chloroformylvaleryl)benzo-15-crown-5 and 4'-(ω -chloroformylheptatanoyl)benzo-15-crown-5.²⁰ PNPP stock solution for kinetics was prepared in acetonitrile.

Synthesis of hydroxamic acids containing benzo-15-crown-5 and their transition-metal complexes. 4'-[ω -(*N*-hydroxy-*N*-phenylaminoformyl)valeryl]benzo-15-crown-5 (**HL**¹): *N*-phenylhydroxylamine (0.44 g, 4 mmol) was dissolved in cold diethyl ether (30 cm³), and the solution was stirred mechanically with external cooling to -5 °C. Powdered NaHCO₃ (0.50 g, 6 mmol) suspended in water (3 cm³) was added to the solution. 4'-(ω -Chloroformylvaleryl)benzo-15-crown-5 (1.66 g, 4 mmol) dissolved in dichloromethane (5 cm³) was added dropwise over a period of 0.5 h. After the addition was completed, the mixture was vigorously stirred for 2 h at 0 °C. The solution was then filtered and the residue was triturated with a saturated solution of sodium bicarbonate in a mortar for 15 min to remove acid impurities. The solid was filtered off and washed with cold water, then recrystallised from ethanol and dried to obtain pure product **HL**¹ as white crystals. 1.02 g, yield 52.3%, m.p. 96–98 °C. ¹H NMR (CDCl₃) δ : 7.53–6.80 (m, 8H, ArH), 4.16–3.74 (m, 16H, OCH₂), 2.88(t, 2H, COCH₂), 2.38(t, 2H, CH₂CON), 1.70–1.61 (m, 4H, 2 \times CH₂)ppm; IR (KBr, cm⁻¹) ν_{\max} : 3206(OH), 2984, 2864, 1452(CH₂), 1670(C=O), 1625(CON), 1592, 1514(Ar), 1276, 1056 (Ar–O–C), 1136(C–O–C), 914(N–O); MS *m/z*: 488(M⁺+1,90). Anal. calcd. for C₂₆H₃₃NO₈: C 64.1, H 6.8, N 2.9; found: C 64.4, H 6.9, N 2.7.

4'-[ω -(*N*-hydroxy-*N*-phenylaminoformyl)heptatanoyl]benzo-15-crown-5(**HL**²): **HL**² was prepared as described for **HL**¹ to give white crystals (0.96 g), yield 46.7%, m.p. 66–67 °C. ¹H NMR (CDCl₃) δ : 7.55–6.87(m, 8H, ArH), 4.14–3.73(m, 16H, OCH₂), 2.90 (t, 2H COCH₂), 2.36(t, 2H, CH₂CON), 1.68(m, 8H, 4 \times CH₂) ppm; IR (KBr, cm⁻¹) ν_{\max} : 3282(OH), 2933, 2875,1433(CH₂), 1673(C=O), 1625(CON), 1593, 1516(Ar), 1273, 1056(Ar–O–C), 1132 (C–O–C), 916(N–O); MS *m/z*: 515(M⁺,25). Anal. Calcd. for C₂₈H₃₇NO₈: C 65.2, H 7.2, N 2.7; found C 65.3, H 7.3.N 2.6.

General methods for preparation of hydroxamic acid complexes

A solution of hydroxamic acids ligands **HL**¹ or **HL**² (2.0 mmol) in EtOH(10 cm³) was added to a solution of M(OAc)₂.4H₂O (1.1 mmol) in EtOH (20 cm³) at 70 °C. The pH of the mixture was adjusted slowly with sodium acetate to precipitate a solid. The mixture was kept at 70 °C for 2 h and the solid was then filtered, washed with water and EtOH, and dried in a vacuum to give the complexes.

CoL¹₂: Pink solid 0.53 g, 51.4% yield, m.p. 184–186 °C. IR (KBr, cm⁻¹) ν_{\max} : 3065(ArH), 2938, 2854(CH₂), 1675(C=O), 1605(CON), 1273(Ar–O–C), 1126(C–O–C), 938(N–O); ESI-MS *m/z*: 1031(M⁺). Anal. calcd. for CoC₅₂H₆₄N₂O₁₆: C 60.5, H 6.2, N 2.7, Co 5.7; found C 60.7, H 6.4, N 2.5, Co 5.6. Λ_m (S cm² mol⁻¹): 3.61.

MnL¹₂: White solid 0.50 g, 48.3% yield, m.p. 179–180 °C. IR (KBr, cm⁻¹) ν_{\max} : 3057(ArH), 2917, 2832(CH₂), 1672(C=O), 1606(CON), 1274(Ar–O–C), 1138(C–O–C), 942(N–O); ESI-MS *m/z*: 1028(M⁺+1). Anal. calcd. for MnC₅₂H₆₄N₂O₁₆: C 60.8, H 6.2, N 2.7, Mn 5.4; found C 60.6, H 6.4, N 2.5, Mn 5.5. Λ_m (S cm² mol⁻¹): 3.34.

CuL¹₂: Light blue solid 0.63 g, 61.1% yield, m.p. 205–207 °C. IR (KBr, cm⁻¹) ν_{\max} : 3059(ArH), 2924(CH₂), 1673(C=O), 1605(CON), 1273(Ar–O–C), 1135(C–O–C), 941(N–O); ESI-MS *m/z*: 1037 (M⁺+1). Anal. calcd. for CuC₅₂H₆₄N₂O₁₆: C 60.2, H 6.2, N 2.7, Cu 6.1; found C 60.4, H 6.3, N 2.5, Cu 6.0. Λ_m (S cm² mol⁻¹): 3.42.

ZnL¹₂: Light grey solid 0.63 g, 57.2% yield, m.p. 197–199 °C. IR (KBr, cm⁻¹) ν_{\max} : 3056(ArH), 2923(CH₂), 1674(C=O), 1604(CON), 1275(Ar–O–C), 1134(C–O–C), 942(N–O); ESI-MS *m/z*: 1038 (M⁺+1). (Anal. calcd. for ZnC₅₂H₆₄N₂O₁₆: C 60.2, H 6.2, N 2.7, Zn 6.3; found C 60.3, H 6.0, N 2.9, Zn 6.1. Λ_m (S cm² mol⁻¹): 3.56.

CoL²₂: Pink solid 0.65 g, 59.7% yield, m.p. 160 °C (dec.). IR (KBr, cm⁻¹) ν_{\max} : 3065(ArH), 2928, 2859(CH₂), 1674(C=O), 1605(CON), 1270(Ar–O–C), 1130(C–O–C), 934(N–O); ESI-MS *m/z*: 1087(M⁺). Anal. calcd. for CoC₅₆H₇₂N₂O₁₆: C 61.8, H 6.6, N 2.6, Co 5.4; found C 61.6, H 6.5, N 2.7, Co 5.6. Λ_m (S cm² mol⁻¹): 3.28.

MnL²₂: White solid 0.57 g, 52.9% yield, m.p. 157–158 °C. IR (KBr, cm⁻¹) ν_{\max} : 3061(ArH), 2943, 2846(CH₂), 1672(C=O), 1606(CON), 1274(Ar–O–C), 1135(C–O–C), 939(N–O); ESI-MS *m/z*: 1084(M⁺+1). Anal. calcd. for MnC₅₆H₇₂N₂O₁₆: C 62.1, H 6.7, N 2.6, Mn 5.1; found C 62.7, H 6.5, N 2.5, Mn 5.3. Λ_m (S cm² mol⁻¹): 3.53.

CuL²₂: Light blue solid 0.64 g, 58.5% yield, m.p. 196–198 °C. IR (KBr, cm⁻¹) ν_{\max} : 3059(ArH), 2924(CH₂), 1673(C=O), 1605(CON), 1271(Ar–O–C), 1135(C–O–C), 942(N–O); ESI-MS *m/z*: 1093

(M⁺+1). Anal. calcd. for CuC₅₂H₆₄N₂O₁₆: C 61.5, H 5.9, N 2.6, Cu 5.8; found C 61.4, H 5.9, N 2.8, Cu 5.8. Λ_m (S cm² mol⁻¹): 3.49.

ZnL²₂: Light grey solid 0.65 g, 59.5% yield, m.p. 197–199 °C. IR (KBr, cm⁻¹) ν_{\max} : 3056(ArH), 2923(CH₂), 1674(C=O), 1603(CON), 1275(Ar–O–C), 1134(C–O–C), 943(N–O); ESI-MS *m/z*: 1094 (M⁺+1). Anal. calcd. for ZnC₅₂H₆₄N₂O₁₆: C 61.5, H 5.9, N 2.6, Zn 6.0; found C 61.4, H 6.0, N 2.5, Zn 6.1. Λ_m (S cm² mol⁻¹): 3.44.

Compared with the IR spectra of the ligand, the IR spectra (ν_{ArH} , ν_{CH_2} , $\nu_{\text{C-O-C}}$) of the complexes are almost at the same frequency, except that the N–O stretching vibration shifts 24–28 cm⁻¹ to higher frequency and its intensity is greater than that of free ligand. This indicates the formation of a N–O...M coordination bond; the absence of an OH stretching vibration (3206 cm⁻¹) in the complexes indicates deprotonation of N–OH of the ligand on complex formation; the NC=O stretching vibration shifts 18–20 cm⁻¹ to lower frequency, this indicates the formation of a C=O...M coordination bond.^{21,22} The C–O–C stretching vibrations in the crown ether ring are almost unchanged. The mass spectra and elemental analysis of the complexes indicate that **HL** forms 2:1(ligand/metal) complexes. The observed molar conductance of all complexes in DMF solution (1.0 \times 10⁻³ mol dm⁻³) at 25 °C also show that they are non-electrolytes.²³

Kinetics studies

Kinetic measurements were made spectrophotometrically at 25 °C and different pH values, employing a GBC 916 UV/Vis spectrophotometer equipped with a thermostatic cell holder. Reactions were initiated by injecting 30–70 μ l of a 2.00 \times 10⁻⁴ mol dm⁻³ stock acetonitrile solution of the desired PNPP into a 1 cm cuvette containing 3 cm³ of buffer solution containing the desired concentration of the complex. The pseudo-first-order rate constants for PNPP hydrolysis were determined by monitoring the release of *p*-nitrophenol at 400 nm under the condition of more than 10-fold excess of substrate over catalyst concentration. The pseudo-first-order rate constants were obtained on fitting an equation $\ln(A_{\infty}-A_{\infty})-\ln(A_0-A_{\infty})=-k_{\text{obs}}t$ by a non-linear least-squares treatment, and its average relative standard deviation is less than 1.5%. The ionic strength of the buffer solutions of all reaction systems was maintained at 0.1 M KNO₃ in the experiment.

Results and discussion

Pseudo-first-order rate constants for catalytic hydrolysis of PNPP at 25 °C

The pseudo-first-order rate constants (k_{obs}) of catalytic PNPP hydrolysis shown in Table 1 were obtained by monitoring the release of *p*-nitrophenol from the substrate at 25 °C. The pseudo-first-order rate constant (k_0) of PNPP hydrolysis in absence of complex is 0.78 \times 10⁻⁵ s⁻¹ at pH = 7.00, 25 °C and [S] = 2.00 \times 10⁻⁴ mol dm⁻³. Compared with k_0 , the pseudo-first-order rate constants (k_{obs}) for the PNPP hydrolysis catalysed by the complexes increase by a factor of ca 10.79 \times 10³ for CuL¹₂, 9.90 \times 10³ for CuL²₂, 6.97 \times 10³ for CoL¹₂, 5.53 \times 10³ for CoL²₂, 2.32 \times 10³ for ZnL¹₂, 1.99 \times 10³ for ZnL²₂, 1.60 \times 10³ for MnL¹₂ and 1.38 \times 10³ for MnL²₂, respectively, at 25 °C, pH = 7.00 and [S] = 2.00 \times 10⁻⁴ mol dm⁻³. Table 1 also shows that the pseudo-first-order rate constants (k_{obs}) of PNPP hydrolysis catalysed by the complexes are 1.38 \times 10³–10.79 \times 10³ times than that of spontaneous hydrolysis of PNPP at pH = 7.00 and [S] = 2.00 \times 10⁻⁴ mol dm⁻³. The catalytic activity of different metal ions in complexes of the same ligand decreased in the order of Cu²⁺>Co²⁺>Zn²⁺>Mn²⁺. From Table 1, the pseudo-first-order rate constants (k_{obs}) for the hydrolysis of PNPP increase with increase of both substrate (PNPP) concentration and the pH value of reaction systems, as exemplified in Fig. 2 for the CoL¹₂ complex catalysing the hydrolysis of PNPP in buffer solution. The bigger the concentration of the substrate (PNPP), the bigger is the concentration of the intermediate formed by the substrate and the active species, which leads to higher reactivity and bigger rate constants.

Kinetics model of catalytic PNPP hydrolysis

The catalytic hydrolysis process of PNPP in aqueous solution of the complexes can be expressed as Scheme 1 involving equations (1) and (2).

Where S is the substrate PNPP, K is the association constant between the substrate and the hydrated complex (ML), MLS represents the intermediate, k is the first-order-rate constant for product formation, and is pH-dependent. k_0 is the pseudo-first-order-rate constant of PNPP hydrolysis in absence of catalyst.

The rate of PNPP spontaneous hydrolysis is much lower than that of catalytic hydrolysis, so the products of PNPP spontaneous

Table 1 Pseudo-first-order rate constants (k_{obs}) of PNPP catalytic hydrolysis in buffer solutions

Complex	10^4 [PNPP] /mol dm ⁻³	$10^2 k_{\text{obs}} (\text{s}^{-1})$				
		pH 7.00	7.30	7.60	7.90	8.20
CuL ₂	2.00	8.42	10.41	16.96	23.76	48.98
	2.67	10.52	13.21	20.73	30.50	63.14
	3.33	12.94	16.65	25.77	36.26	80.13
	4.00	14.98	18.79	31.20	43.19	91.20
	4.67	16.95	22.17	36.46	53.62	103.07
CoL ₂	2.00	5.44	7.46	13.94	22.26	45.98
	2.67	6.59	9.61	17.63	26.40	57.74
	3.33	7.81	11.62	20.57	32.56	72.13
	4.00	9.48	13.19	24.40	37.19	76.10
	4.67	10.53	15.27	28.66	48.40	97.07
ZnL ₂	2.00	1.81	3.49	7.76	19.24	40.85
	2.67	2.32	4.47	9.02	24.63	49.25
	3.33	2.90	5.50	11.20	28.91	58.38
	4.00	3.32	6.41	13.52	34.54	69.26
	4.67	3.92	7.52	17.26	38.93	79.59
MnL ₂	2.00	1.25	2.95	5.86	14.74	31.05
	2.67	1.56	3.53	7.77	18.53	41.25
	3.33	1.92	4.40	9.20	22.91	47.38
	4.00	2.30	5.19	10.21	25.04	56.26
	4.67	2.71	6.53	12.19	29.55	65.69
CuL ₂ ²	2.00	7.72	9.18	13.53	20.74	43.16
	2.67	9.77	12.26	17.50	26.86	54.62
	3.33	11.83	14.55	21.08	33.51	67.43
	4.00	13.49	16.75	24.76	37.29	77.50
	4.67	14.86	19.10	28.57	45.06	89.12
CoL ₂ ²	2.00	4.31	5.99	9.38	16.54	38.02
	2.67	5.30	7.94	12.64	19.86	45.22
	3.33	6.50	9.35	14.58	24.09	56.43
	4.00	7.49	10.80	16.86	29.79	67.50
	4.67	8.45	12.30	19.97	35.51	79.12
ZnL ₂ ²	2.00	1.55	2.98	6.46	15.02	34.83
	2.67	1.99	3.77	8.18	18.65	43.50
	3.33	2.45	4.46	9.94	23.79	52.82
	4.00	2.84	5.47	11.49	26.17	61.86
	4.67	3.31	6.51	13.75	30.14	68.16
MnL ₂ ²	2.00	1.08	2.62	5.49	14.92	28.58
	2.67	1.44	3.47	6.34	16.38	37.25
	3.33	1.68	3.81	8.14	20.79	44.38
	4.00	2.00	4.37	9.66	24.57	52.26
	4.67	2.29	6.11	11.42	27.62	58.69

 Condition: 25 ± 0.1 °C, $I = 0.1$, [complex] = 1.00×10^{-5} mol dm⁻³.

hydrolysis can be neglected in kinetics calculation. Hence, Scheme 1 can lead to the rate equation:

$$\text{Rate} = k [\text{MLS}] \quad (3)$$

 The association constants K can be expressed in terms of concentrations:

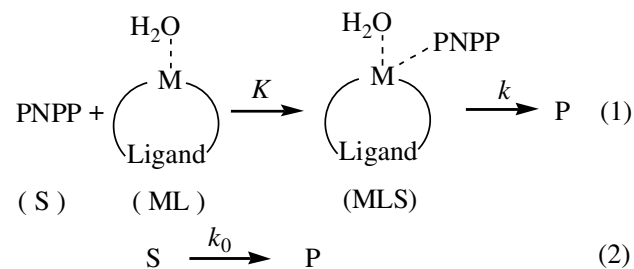
$$K = [\text{MLS}] / [\text{ML}][\text{S}] \quad (4)$$

According to the material balance, we have:

$$[\text{ML}]_{\text{T}} = [\text{ML}] + [\text{MLS}] \quad (5)$$

Combination of equation (4) and (5) leads to:

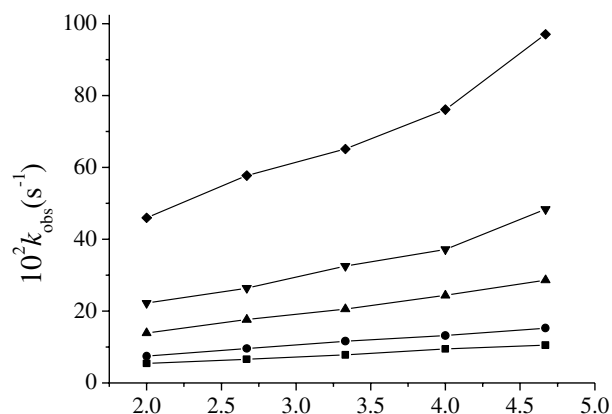
$$[\text{MLS}] = \frac{K[\text{S}][\text{ML}]_{\text{T}}}{1 + K[\text{S}]} \quad (6)$$


Scheme 1

Combination of equation (6) and (3) gives:

$$\text{rate} = \frac{kK[\text{S}][\text{ML}]_{\text{T}}}{1 + K[\text{S}]} = k_{\text{obs}} [\text{ML}]_{\text{T}} \quad (7)$$

$$k_{\text{obs}} = \frac{kK[\text{S}]}{1 + K[\text{S}]} \quad (8)$$


Fig. 2 The pseudo-first-order rate constants (k_{obs}) of catalytic PNPP hydrolysis for CoL_2 complex in buffer solution at 25 °C, ■ pH 7.00 ● pH 7.30 ▲ pH 7.60 ▼ pH 7.90 ◆ pH 8.20.

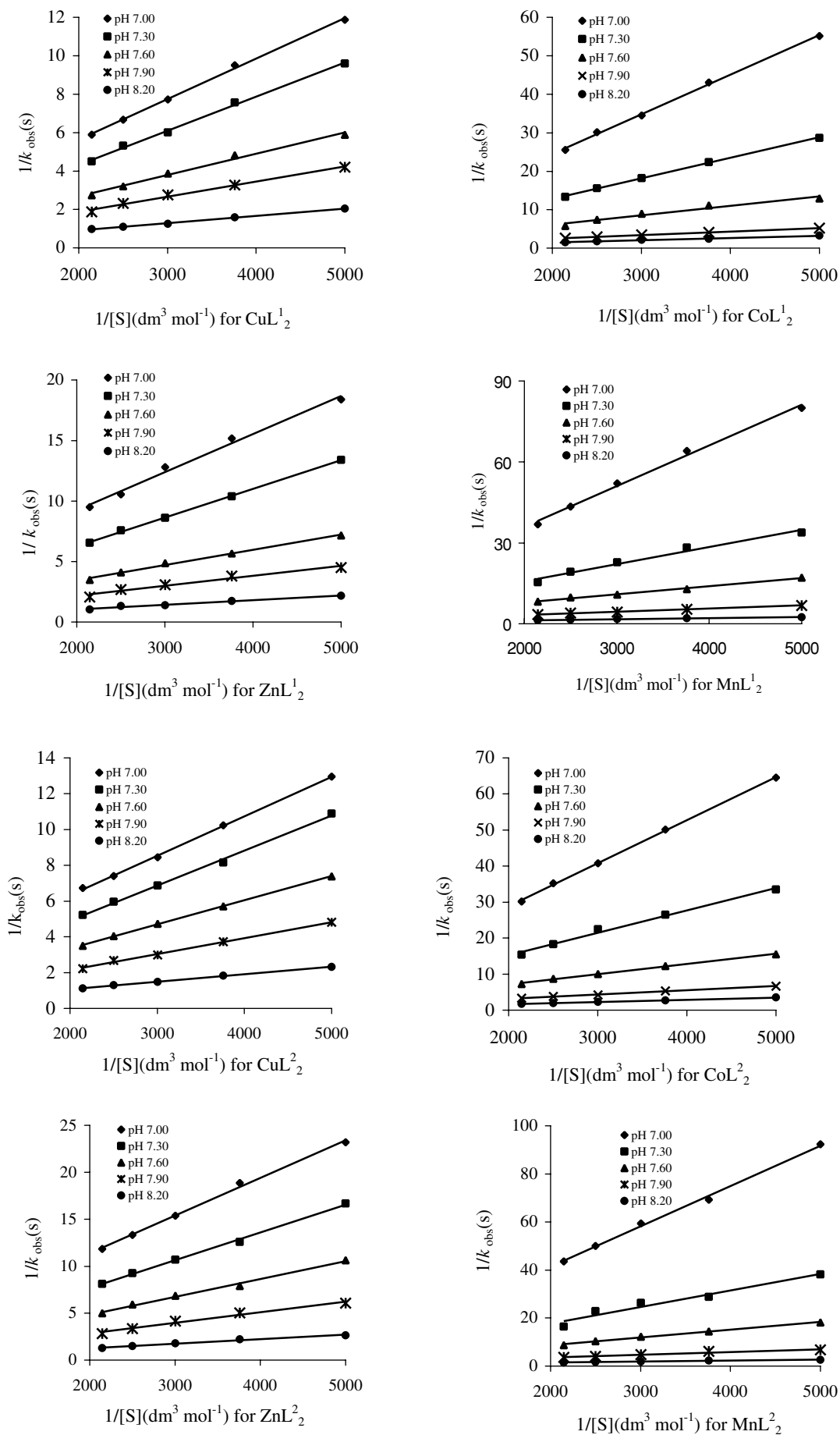


Fig. 3 Effect of substrate concentration on first-order-rate constants for the catalytic hydrolysis of PNPP by the complexes CuL_2 , CuL_2^2 , CoL_2 , CoL_2^2 , ZnL_2 , ZnL_2^2 , MnL_2 and MnL_2^2 at 25 °C in the buffer solution.

Rearrangement of equation (6) gives:

$$\frac{1}{k_{\text{obs}}} = \frac{1}{k} + \frac{1}{Kk[S]} \quad (9)$$

In the above equations, $[ML]$ and $[ML]_T$ are the free and the total concentration of the active species, respectively; $[S]$ is the concentration of free substrate and can be substituted by the initial concentration of the substrate; $[MLS]$ is the concentration of the intermediate formed by the substrate and the active species in the buffered solution.

Based on equation (9), a linear plot, *i.e.*, $1/k_{\text{obs}}$ versus $1/[S]$ is obtained for the ML_2 complexes, respectively, by changing concentration of substrate (see Fig. 3), and these plots allowed the evaluation of K and k , and the results of calculation are summarised in Table 2. Table 2 shows the rate of the PNPP catalytic hydrolysis increases largely with the increase of the pH of the reaction systems from 7.00 to 8.20. It may be due to H_2O being synergically activated by the crown ether ring and central metal ion of complexes.

From Table 2, the association constants (K) in all systems studied enhanced clearly with increasing in the pH values of the buffer solution, which is favourable to the increase of the first-order-rate constant (k) for the hydrolysis of PNPP. In other words, for the same complex, the bigger the association constants, the tighter the association between the substrate and the complex, which leads to higher reactivity and rate constants (k), because the PNPP catalytic hydrolysis is an intramolecular nucleophilic reaction.²⁴

pH-rate profile of catalytic PNPP hydrolysis

It is a known fact that enzymatic activity is changed depending on the acidity of the reaction system. The spatial conformation of the enzyme may be transformed following the changes of the acidity of the reaction system, and the stability of the intermediate (MLS) should also be changed. From the results obtained, it is clear that the first-order-rate constant (k) is pH-dependent. In other words, k is related to the acid dissociation constant K_a of H_2O coordinated to the metal (II) ion. The k value increases along with the increase of the pH value from 7.00 to 8.20. This implies that the reaction process

contains proton transfer at the rate determining step in Scheme 1. This process can be shown as Scheme 2.

K_a is the acidic dissociation constant of H_2O coordinated to the metal ion; k_1 is the first-order-rate constant, which is pH-independent. In this process, the intermediate MLS was ionised or generated proton transfer. The rate for PNPP catalytic hydrolysis depends on the stabilisation of the intermediate MLS^- . According to the principles of the chemical equilibration, it is favourable for the intermediate MLS to form the intermediate MLS^- and generate the products (P) in alkaline solution. Hence, the first-order-rate constants (k) increase with increasing of pH value in the reaction system.

Due to the chemical balance principle, we have:

$$K_a = [H^+][MLS^-]/[MLS] \quad (10)$$

According to the material balance, we have:

$$[MLS] = [MLS]_t + [MLS^-] \quad (11)$$

Combination of equations (10) and (11) leads to:

$$[MLS^-] = \frac{K_a [MLS]}{[H^+] + K_a} \quad (12)$$

The rate equation in Scheme 2 can be expressed as:

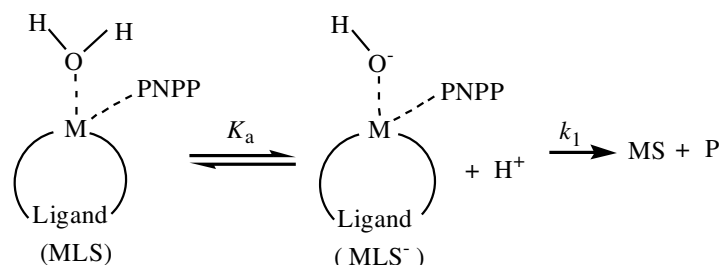
$$k[MLS] = k_1 [MLS^-] \quad (13)$$

Combination of equations (12) and (13) leads to:

$$k = \frac{K_a k_1}{[H^+] + K_a} \quad (14)$$

Rearrangement of equation (14) gives:

$$\frac{1}{k} = \frac{1}{k_1} + \frac{1}{k_1 K_a} [H^+] \quad (15)$$



Scheme 2

Table 2 K and k of the catalytic hydrolysis of PNPP by ML_2 complexes in buffer solution

complex	pH	$k(s^{-1})$	$10^{-2}K(\text{mol dm}^{-3})$	complex	pH	$k(s^{-1})$	$10^{-2}K(\text{mol dm}^{-3})$
CuL ₂	7.00	0.71	3.44	CuL ₂	7.00	0.52	3.90
	7.30	1.27	3.56		7.30	0.99	4.57
	7.60	2.13	4.21		7.60	1.56	5.07
	7.90	3.45	4.29		7.90	2.86	5.87
	8.20	7.14	6.77		8.20	4.35	8.81
CoL ₂	7.00	0.34	3.77	CoL ₂	7.00	0.30	4.18
	7.30	0.65	3.81		7.30	0.56	4.26
	7.60	1.09	5.03		7.60	1.00	5.28
	7.90	1.87	6.99		7.90	1.71	5.88
	8.20	3.74	7.29		8.20	3.46	6.73
ZnL ₂	7.00	0.26	6.38	ZnL ₂	7.00	0.20	5.26
	7.30	0.50	6.66		7.30	0.37	5.31
	7.60	0.83	6.69		7.60	0.68	5.78
	7.90	1.59	7.39		7.90	1.23	5.94
	8.20	3.23	9.53		8.20	2.86	8.42
MnL ₂	7.00	0.17	3.96	MnL ₂	7.00	0.13	4.73
	7.30	0.34	4.55		7.30	0.26	5.53
	7.60	0.53	6.36		7.60	0.44	6.80
	7.90	1.07	7.78		7.90	0.73	12.48
	8.20	2.40	10.38		8.20	1.53	16.38

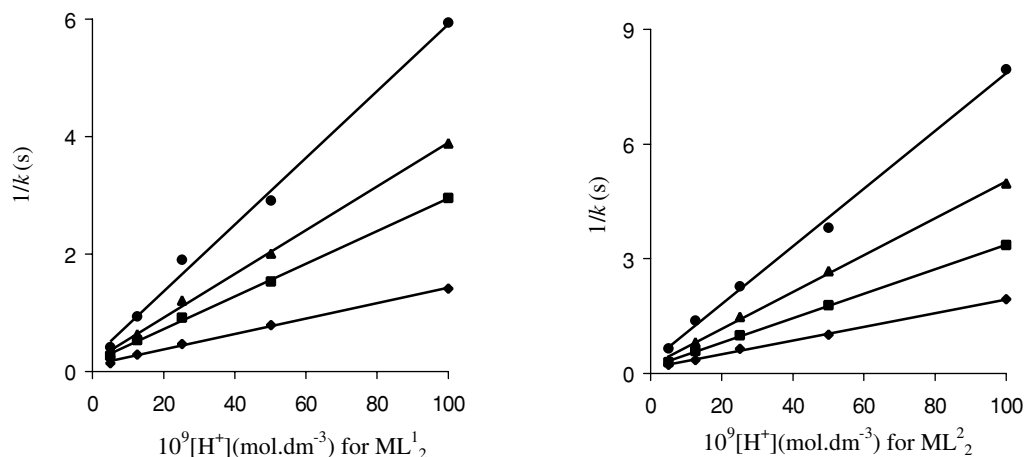


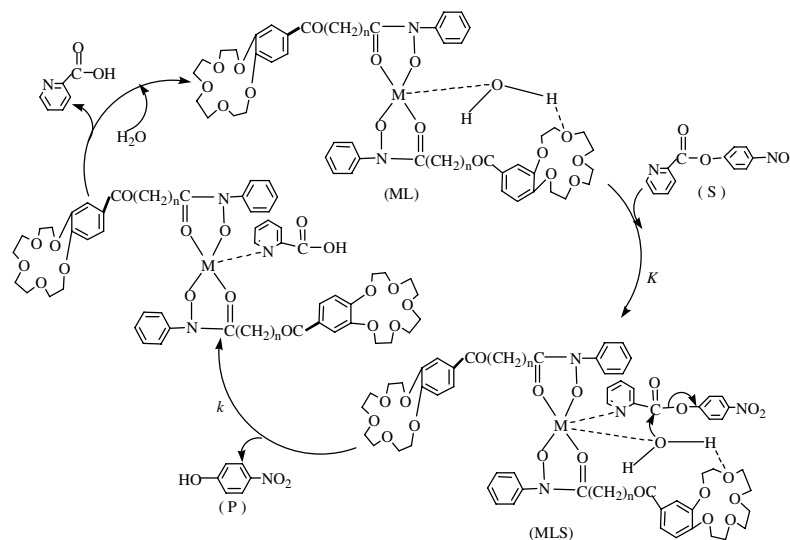
Fig. 4 pH-rate profile for the catalytic hydrolysis of PNPP by the complexes at 25 °C in the buffer solution (◆CuL₂ ■CoL₂ ▲ZnL₂ ●MnL₂)

[MLS] is the dissociated concentration of the intermediate MLS, [MLS]₁ is the undissociated concentration of the intermediate MLS. On the basis of equation (15), the k_1 and K_a values can be obtained from the slope and the intercept of the plot $1/k$ versus $[H^+]$. The results are shown in Figure 4 and Table 3.

From the results in Fig. 4 and Table 3, the first-order-rate constants (k_1) follow the order Cu(II)>Co(II)>Zn(II)>Mn(II) with the same ligands. In a metal-centred hydrolysis, the pK_a of a coordinated water molecule is dramatically lowered by a metal centre of a high Lewis acidity and is a key factor for the activity. This coordinated water thus become a good nucleophile in the form of hydroxide around neutral pH for the attack at the substrate PNPP, as observed in metallohydrolases.²⁵ Therefore, from Table 3, the pK_a values for these divalent metal complexes studied mean that the water molecules bound to metal ions can easily be deprotonated to hydroxyl groups acting as nucleophiles in buffer solution with neutral pH values. The pK_a values follow the order Cu(II)<Co(II)<Zn(II)<Mn(II) with the same ligand. The relatively low pK_a values might be attributed to a relatively high Lewis acidity of central metal ions in complexes, which follow the order Cu(II)>Co(II)>Zn(II)>Mn(II).

Effects of the complex structure on the rate of catalytic PNPP hydrolysis

It is well known that the enzymatic catalytic activity and selectivity are correlated to the enzymatic structure. The synthetic hydrolase used in this paper exhibits the effects of structure similar to that of the natural hydrolase. From Table 3, it can be seen that the catalytic activity of the complexes followed the order Cu(II)>Co(II)>Zn(II)>Mn(II) due to the central metal ion radius, which follow the order Cu(II) <Co(II)<Zn(II)<Mn(II). The smaller the central metal ion radius is, the stronger is its ability to activate H₂O and bind PNPP, with the result that the rate of catalytic PNPP hydrolysis is larger. On the other hand, the pseudo first-order-rate constants (k_{obs}) followed the order ML¹₂>ML²₂, which may be attributed to the structural difference between ligands HL¹ and HL². The distance of crown ether ring and central metal ion is shorter in complex HL¹ than in HL², therefore, the ability of H₂O being synergically activated by the crown ether ring and central metal ion of complexes is stronger in ML¹₂ than in ML²₂. This can promote deprotonation of water molecules bound to metal ions to hydroxyl groups acting as nucleophiles forming the intermediate MLS (see Scheme 3).



Scheme 3 Proposed mechanism for hydrolysis of PNPP catalysed by transition-metal hydroxamate containing benzo-15-crown-5.

Table 3 k_1 and pK_a of the catalytic hydrolysis of PNPP by ML₂ complexes in buffer solution

Complexes	k_1 (s)	pK_a	complexes	k_1 (s)	pK_a
CuL ₂ ¹	8.73	8.06	CuL ₂ ²	6.97	8.07
CoL ₂ ¹	6.41	8.25	CoL ₂ ²	6.03	8.29
ZnL ₂ ¹	5.72	8.33	ZnL ₂ ²	5.03	8.39
MnL ₂ ¹	4.38	8.40	MnL ₂ ²	3.27	8.46

Table 4 Apparent activation energy (E_a) values of the catalytic hydrolysis of PNPP by ML₂ complexes in buffer solution

Complexes	E_a (kJ mol ⁻¹)	Complexes	E_a (kJ mol ⁻¹)
CuL ₂ ¹	13.87	CuL ₂ ²	14.23
CoL ₂ ¹	14.96	CoL ₂ ²	15.41
ZnL ₂ ¹	16.29	ZnL ₂ ²	16.47
MnL ₂ ¹	16.79	MnL ₂ ²	17.18

Effect of temperature and apparent activation energy on catalytic PNPP hydrolysis

The effects of temperature on enzyme catalysis hydrolysis appeared similar to the affect of acidity of the reaction system. In order to investigate the effect of temperature on catalytic hydrolysis, the pseudo-first-order-rate constants (k_{obs}) of PNPP hydrolysis were obtained at five different temperatures from 15 to 55 °C. According to the Arrhenius formula: $-\ln k_{\text{obs}} = E_a/RT + A$, straight lines for $-\ln k_{\text{obs}}$ versus $1/T$ are obtained. The apparent activation energy (E_a) values that can be obtained from the slopes of the straight lines are shown in Table 4.

From Table 4, the apparent activation energy E_a values followed the order Cu(II)<Co(II)<Zn(II)<Mn(II) with the same ligand. This indicates that eight complexes are stable in the temperature range investigated. Since the formation rate of the intermediate, MLS and MLS⁻, should increase along with rise of the reactive temperature, the rate of PNPP catalytic hydrolysis is enhanced.

Proposed mechanism of catalytic PNPP hydrolysis by transition-metal hydroxamate containing benzo-15-crown-5

The proposed mechanism of the catalytic hydrolysis of PNPP by ML₂ is outlined in Scheme 3 on the basis of previous reports²⁶ and pK_a values of complexes above. According to the complex structure, H₂O could be coordinated to the metal ion, which would result in the forming of a hydrated complex in aqueous solution. This hydrated complex may be the real active species for the PNPP catalytic hydrolysis.²⁷ Therefore, we assume that the mechanism of PNPP catalytic hydrolysis is similar to the hydrolytic reaction catalysed by a hydrolytic metalloenzyme.

Scheme 3 shows that: (1) H₂O coordinated to metal ion is activated synergistically by the central metal ion and crown ether ring, which endow special performance and characteristics due to the hydrophobicity of the outer ethylene groups and the orderly arrangement of inner oxygen atoms,^{28,29} and then the intramolecular hydroxide is generated; (2) the N atom of the pyridine ring in the PNPP molecule is coordinated to the metal ion in the complex, forming the intermediate MLS; (3) active H₂O carries out intramolecular attack on the positive C atom of the ester carbonyl group in the PNPP molecule to promote the departure of the formed *p*-nitrophenol with a first-order-rate constant (k), which is the step determining rate of the total reaction; (4) a picoline acid molecule coordinated to the metal ion is released and H₂O is bonded to the metal ion quickly again.

Conclusions

We have investigated the catalytic hydrolysis of carboxylic esters (PNPP) by transition metal hydroxamates (Cu²⁺, Co²⁺, Zn²⁺, Mn²⁺) containing benzo-15-crown. The results show that the rate of catalytic PNPP hydrolysis is influenced by the formation rate of the intramolecular hydroxide of the intermediate; the pseudo-first-order rate constants (k_{obs}) of PNPP hydrolysis catalysed by the complexes is 1.38×10^3 – 10.79×10^3 times than that of spontaneous hydrolysis of PNPP at pH = 7.00 and [S] = 2.00×10^{-4} mol dm⁻³; the catalytic activity of different metal ion deceased in the order of Cu(II)>Co(II)>Zn(II)>Mn(II); the rate of the catalytic PNPP hydrolysis increases largely with the increase of the pH from 7.00 to 8.20; the apparent activation energy (E_a) of the catalytic PNPP hydrolysis follow the order Cu(II)<Co(II)<Zn(II)<Mn(II) under the same ligand. The studies also indicate that eight complexes are stable in the temperature range and the acidity range investigated.

The authors gratefully acknowledge financial support from China National Natural Science Foundation (No: 20072025).

Received 16 January 2005; accepted 11 July 2005
Paper 05/3018

References

- 1 L. Hegg and J.N. Burstyn, *Coord. Chem. Rev.*, 1998, **173**, 133.
- 2 P. Molenveld, J.F.J. Engbersen and D.N. Reinhoudt, *Chem. Soc. Rev.*, 2000, **29**, 75.
- 3 R. Fornasier, P. Scrimin, P. Tecilla and U. Tonellato, *J. Am. Chem. Soc.*, 1989, **111**, 224.
- 4 B. Jiang, B.Y. Jiang, X.Q. Yu and X.C. Zeng, *Langmuir*, 2002, **18**, 6769.
- 5 T. Fujita, Y. Inaba, K. Ogino and W. Tagaki, *Bull. Chem. Soc. Jpn.*, 1988, **62**, 1661.
- 6 X. Xiang, X.O. Yu and R.G. Xie, *J. Mol. Catal. A: Chemical*, 2002, **187**, 195.
- 7 P. Molenveld, S.Kapsabelis and J.F.J. Engbersen, *J. Am. Chem. Soc.*, 1997, **119**, 2948.
- 8 R. Breslow and E. Kool, *Tetrahedron Lett.*, 1988, **29**, 1635.
- 9 J.Z. Li, J.Q. Xie, W. Zeng and S.Y. Qin, *Transition Met. Chem.*, 2004, **29**, 488.
- 10 X.M. Kou, S.Q. Cheng, J. Du and X.C. Zeng, *J. Mol. Catal. A: Chemical*, 2004, **210**, 23.
- 11 J.C. Powers and J.W. Harper, *Review on Hydroxamic Acid as Metalloprotease Inhibitors in Protease Inhibitors*, eds. A.J. Barrett, G. Salvesan, Marcel Dekker, New York, 1986, p. 219.
- 12 M.J. Miller, *J. Chem. Rev.*, 1989, **89**, 1563.
- 13 A.L. Crumbliss, *Coord. Chem. Rev.*, 1990, **105**, 155.
- 14 S. Hashimoto, R. Yamashita and Y. Nakamura, *Chem. Lett.*, 1992, 639.
- 15 D.J. Berrisford, C. Bolm and K.B. Sharpless, *Angew. Chem., Int. Ed. Engl.*, 1995, **34**, 1059.
- 16 H. Yang, S.Y. Qin and X.X. Lu, *Chin. Chem. Lett.*, 1999, **10**, 79.
- 17 H.B. Li, Y. Du, X.Y. Wei and S.Y. Qin, *Acta Chim. Sinica*, 2002, **60**, 886.
- 18 F. Vernon and H.D. Gunawardhana, *Anal. Chem. Acta*, 1978, **98**, 349.
- 19 D.S. Sigman and C.T. Jorgensen, *J. Am. Chem. Soc.*, 1972, **94**, 1724.
- 20 H.B. Li, *Ph. D. Dissertation*, Sichuan University, 2002.
- 21 D.R. Agrawal and S.G. Tandon, *J. Ind. Chem. Soc.*, 1971, **48**, 571.
- 22 A. Syamal and V.D. Ghanekar, *Acta Chim. Acad. Sci. Hung.*, 1977, **93**, 43.
- 23 W.J. Geary, *Coord. Chem. Rev.*, 1971, **7**, 81.
- 24 B.Y. Jiang, Y. Xiang, J. Du, J.Q. Xie, C.W. Hu and X.C. Zeng, *Colloids Surf. A*, 2004, 235, 145.
- 25 W.N. Lipscomb and N. Sträter, *Chem. Rev.*, 1996, **96**, 2375.
- 26 R. Hettich and H.J. Schneider, *J. Am. Chem. Soc.*, 1997, **119**, 5638.
- 27 E. Kimura, H. Hashimoto and T. Koike, *J. Am. Chem. Soc.*, 1996, **118**, 10963.
- 28 H. Hochisako, H. Ihara, J. Kamiya, C. Hirayama and K. Yamnda, *Chem. Commun.*, 1997, 19.
- 29 A. Galon, D. Andreu, A.M. Echavarren, P. Prades and J. de. Mendoza, *J. Am. Chem. Soc.*, 1992, **119**, 5638.